

Structure of a (μ -Oxo)(dihydroxo)diiron(III) Complex and Its Reactivity toward Phosphodiester

Carole Duboc-Toia,[†] Stéphane Ménage,^{*†} Jean-Marc Vincent, Marie Thérèse Averbuch-Pouchot, and Marc Fontecave[‡]

Laboratoire d'Etudes Dynamiques et Structurales de la Sélectivité (UMR CNRS 5616), Université J. Fourier, BP53X, 38041 Grenoble, France

Received September 18, 1997

Functional models for nonheme diiron proteins have received much attention during the recent years. Some (μ -oxo)diiron(III) complexes were reported as catalysts for oxidations,¹ thus modeling the activity of the diiron centers of methane monooxygenase,² desaturase,³ and ribonucleotide reductase.⁴ No relevant functional models for purple acid phosphatase (PAP),⁵ containing an Fe^{III}Fe^{II} active center, have been reported so far. Recently, hydration of acetonitrile by diiron(III) complexes was performed.^{6,7} The key role of a coordinated hydroxide, acting as a nucleophile, and the activation of acetonitrile by ligation to the metal center have been demonstrated. In the course of our effort to model such enzyme activities, we have undertaken a general structure/reactivity study of a series of (μ -oxo)diiron(III) species. Here, we report a study of the acid/base properties of Fe₂O(Phen)₄(OH)₂(NO₃)₄,⁸ **1**. The characterization of the first (μ -oxo)(dihydroxo)diferic complex stable in aqueous medium allowed us to investigate the hydrolytic properties of iron-bound hydroxides.

Spectrophotometric titration of **1** by imidazole or NaOH in water showed the formation of a new stable species **2** upon addition of 2 equiv of base, the green solution turning red. Both charge transfer bands at 580 ($\epsilon = 0.16 \text{ mM}\cdot\text{cm}^{-1}$) and 365 nm

(10 mM $\cdot\text{cm}^{-1}$), characteristic of complex **1**, shifted to 540 (shoulder, 0.10 mM $\cdot\text{cm}^{-1}$) and 350 nm (8.0 mM $\cdot\text{cm}^{-1}$) respectively, suggesting the presence of a stronger electron-donating ligand in the diferric unit.⁹ Proton resonances between 0 and 30 ppm in the ¹H NMR spectrum and the absence of an EPR signal as well confirmed that the (μ -oxo)diiron(III) core was retained in solution. The transformation is reversible since **1** was quantitatively re-formed when perchloric acid or acetic acid was added to complex **2**. Complex **2**, Fe₂O(Phen)₄(OH)₂(NO₃)₂, could be isolated as red crystals by allowing the solution to stand for 1 day.¹⁰

The X ray structure of the cation of **2**·8H₂O¹¹ is shown in Figure 1. The iron atoms are each coordinated by four nitrogen atoms provided by two phenanthroline ligands and by the oxygen atom of the bridge [Fe–O1 = 1.788(1) Å]. The sixth coordination site is occupied by an oxygen atom from a hydroxo ligand. The Fe–OH bond lengths in **2** [1.896(5) Å] are shorter than the Fe–OH₂ bond lengths in **1** [2.027(9) and 2.021(5) Å],⁸ reflecting the higher basicity of the hydroxo ligand. They are in the range of the Fe–OH bond lengths recently reported.^{6,12} Each hydroxo ligand is hydrogen-bonded to a lattice water molecule.

Thus, reaction of complex **1** with a base involves deprotonation of coordinated water molecules, exclusively, with no degradation of the dinuclear unit. Furthermore, potentiometric titration of complex **1** demonstrated the presence of two successive titratable protons with pK_a values of 5.00(10) and 6.85(10), respectively (see Supporting Information). This showed that complex **1** behaved as a diacid in solution (Figure 2). Complex **3**, its base conjugate, is supposed to contain one water molecule on one iron and one hydroxo ligand on the adjacent iron. Spectroscopic studies of complex **1** at pH 6 confirmed that complex **3** retained the dinuclear structure and is structurally analogous to Fe₂O(TPA)₂(H₃O₂)(ClO₄)₃ (see Figure 2).⁶

Hydrolysis of 100 μM bis(2,4-dinitrophenyl) phosphate (BDNPP)¹³ was promoted at 50 °C by 13 μM complex **1** in 50 mM buffered solution as shown by the formation of 2,4-dinitrophenolate. Initial rate constants *k*_{obs} were pH dependent, rising from low pH to reach a maximum at pH 6.0 and then

- * Corresponding author. E-mail: menage@cbrb.ceng.cea.fr.
[†] New address: Laboratoire Chimie et Biologie des Centres Redox Biologiques, DBMS/CB-CEA Grenoble/ CNRS/ Université Joseph Fourier, 17 rue des Martyrs, 38054 Grenoble Cedex 9, France.
[‡] Fontecave, M. *Angew. Chem., Int. Ed. Engl.* **1996**, *35*, 2353–3254.
 (1) MMO models: (a) Kim, J.; Harrison, R. G.; Kim, C.; Que, L., Jr. *J. Am. Chem. Soc.* **1996**, *118*, 4373–4379 and references therein. (b) Ménage, S.; Vincent, J.-M.; Lambeaux, C.; Fontecave, M. *J. Mol. Catal. A: Chem.* **1996**, *113*, 61–75 and references therein. RNR mimics: (c) Ménage, S.; Galey, J. B.; Hussler, G.; Seité, M.; Fontecave, M. *Angew. Chem., Int. Ed. Engl.* **1996**, *35*, 2353–3254. (d) Goldberg, D. P.; Watton, S. P.; Masschelein, A.; Wimmer, L.; Lippard, S. J. *J. Am. Chem. Soc.* **1993**, *115*, 5346–5347. Δ^9 -Desaturase model: (e) Kim, C.; Dong, Y.; Que, L., Jr. *J. Am. Chem. Soc.* **1997**, *119*, 3635–3636.
 (2) (a) Rosenzweig, A. C.; Frederick, C. A.; Lippard, S. J.; Nordlund, P. *Nature* **1993**, *366*, 537–543. (b) Rosenzweig, A. C.; Nordlund, P.; Takahara, P. M.; Lippard, S. J. *Chem. Biol.* **1995**, *2*, 409–418. (c) Wallar, B. J.; Lipscomb, J. D. *Chem. Rev.* **1996**, *96*, 2625–2657 and references cited therein.
 (3) Shanklin, J.; Whittle, E.; Fox, B. G. *Biochemistry* **1994**, *33*, 12787–12794.
 (4) (a) Nordlund, P.; Sjöberg, B.-M.; Eklund, H. *Nature* **1990**, *345*, 593–598. (b) Fontecave, M.; Nordlund, P.; Eklund, H.; Reichardt, P. In *Advances in Enzymology and Related Areas of Molecular Biology*; Meister, A., Ed.; John Wiley and Sons: New York, 1992; Vol. 65, pp 147–183. (c) Stubbe J. In *Advances in Enzymology and Related Areas of Molecular Biology*; Meister, A., Ed.; John Wiley and Sons: New York, 1990; Vol. 63, pp 349–420.
 (5) (a) Vincent, J. B.; Averill, B. A. *FASEB J.* **1990**, *4*, 3009. (b) Doi, K.; Antanaitis, B. C.; Aisen, P. *Struct. Bonding* **1988**, *70*, 1–26. (c) True, A. E.; Que, L., Jr. *Prog. Inorg. Chem.* **1990**, *38*, 97–200. (d) David, S. S.; Que, L., Jr. *J. Am. Chem. Soc.* **1990**, *112*, 6456–6463. (e) Hendry, P. H.; Sargeson, A. M. *Prog. Inorg. Chem.* **1990**, *38*, 201–258.
 (6) (a) Wilkinson, E. C.; Dong, Y.; Que, L., Jr. *J. Am. Chem. Soc.* **1994**, *116*, 8394–8395. (b) Hazell, A.; Jensen, K. B.; McKenzie, C. J.; Toftlund, H. *Inorg. Chem.* **1994**, *33*, 3127–3134.
 (7) Preliminary results indicate the possible hydrolysis of triphenyl phosphate by [(TPA)₂Fe₂O(H₃O₂)](ClO₄)₃. See ref 6b.
 (8) Complex **1** was prepared as described in: Plowman, J. E.; Loehr, T. M.; Schauer, C. K.; Anderson, O. P. *Inorg. Chem.* **1984**, *23*, 3553–3559.

- (9) Ménage, S.; Que, L., Jr. *New J. Chem.* **1990**, *15*, 431–438 and references therein.
 (10) Crystallization was optimal from a 20 mM solution of complex **1** in the presence of 2 equiv of imidazole. Elemental analysis satisfied the following formula: Fe₂O(OH)₂(C₁₂H₈N₂)₄(NO₃)₂·8H₂O. Anal. Calc for C₄₈H₅₀Fe₂N₁₀O₁₇: C, 50.12; H, 4.34; N, 12.20; Fe, 9.70. Found: C, 50.14; H, 4.12; N, 12.74; Fe, 8.54. ¹H NMR in D₂O (δ , ppm): 17.1, 15.0 (H_{\beta}); 8.4, 7.4 (H_{\gamma}); 11.4, 10.2 (H_{\delta}). This spectrum is different from that of complex **1**.
 (11) Crystal data: [Fe₂(μ -O)(C₁₂H₈N₂)₄(OH)₂](NO₃)₂·8H₂O, elongated red prisms, 0.32 × 0.32 × 0.64 mm, monoclinic, space group C2/c (No. 15), *a* = 12.874(5) Å, *b* = 24.584(8) Å, *c* = 18.411(8) Å, β = 92.62(4)°, *V* = 5821(4) Å³, *Z* = 4, μ (Mo K α) = 0.5895 mm⁻¹. For 2955 unique, observed reflections collected at 294 K with *I* > 2 σ (*I*) and 453 refined parameters, the current discrepancy indices are *R* = 0.063, *R*_w = 0.07 (direct methods with TEXSAN software).
 (12) Rapta, M.; Kamaras, P.; Brewer, G.; Jameson, G. B. *J. Am. Chem. Soc.* **1995**, *117*, 12865–12866.
 (13) Bunton, C. A.; Farber, S. J. *J. Org. Chem.* **1969**, *34*, 767–772.

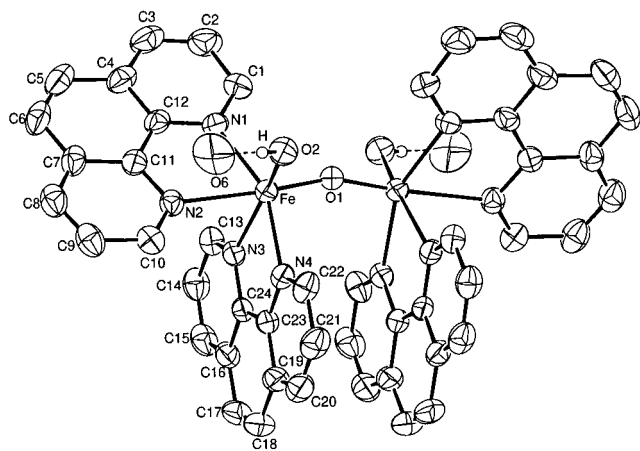


Figure 1. Core structure of complex **2** showing numbering scheme. Selected distances (Å) and angles (deg): Fe–O1, 1.788(1); Fe–O2, 1.896(5); Fe–N1, 2.157(1); Fe–N2, 2.305; Fe–N3, 2.248; Fe–N4, 2.164; O1–Fe–O2, 101.7(2); O1–Fe–N1, 95.2(2); O1–Fe–N2, 166.6(1); O1–Fe–N3, 91.0(2); O1–Fe–N4, 101.7(2); O2–Fe–N1, 98.4(2); O2–Fe–N2, 88.3(2); O2–Fe–N3, 98.4(2); O2–Fe–N4, 94.9(2); N2–Fe–N4, 86.2(2); N1–Fe–N2, 73.5(2); N1–Fe–N3, 88.3(2); N1–Fe–N4, 155.3(2); N2–Fe–N3, 80.6(2); N3–Fe–N4, 74.3(2); Fe···Fe, 3.530(2); Fe–O–Fe, 161.7. O6 corresponds to the lattice water molecule involved in the hydrogen bond with the hydroxo ligand. All hydrogen atoms and the nitrate anions, except the one bound to the hydroxo oxygen atom O2, are omitted for clarity.

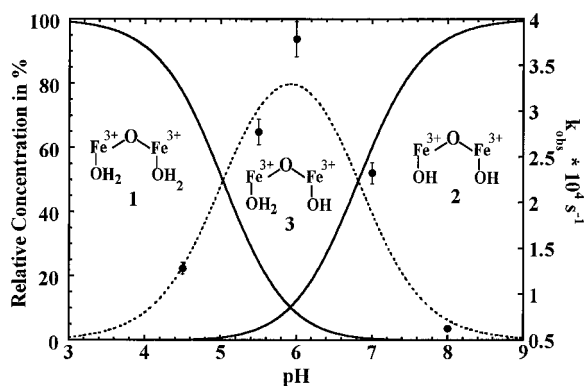


Figure 2. Relative concentrations of complexes **1** (—), **2** (---), and **3** (····) as a function of pH (calculated from potentiometric titration). k_{obs} values for 2,4-dinitrophenolate ($\epsilon = 19\,100\text{ cm}^{-1}\text{ M}^{-1}$) release during reaction of complex **1** with BDNPP as a function of pH (black circles) were determined spectrophotometrically (Supporting Information). Experimental conditions: $T = 50\text{ }^{\circ}\text{C}$, [BDNPP] = $100\text{ }\mu\text{M}$, [complex] = $13\text{ }\mu\text{M}$, 50 mM buffered solution [acetate (pH 4.5), MES (pH range 5–6), and HEPES (pH range 7–8)].

falling off. The resulting bell curve remarkably matched the pH-dependent relative concentration curve of complex **3**, demonstrating that complex **3** was the active species during the hydrolytic reaction (Figure 2). At the optimal pH, the k_{obs} value was linearly correlated with the concentration of complex **1** between $17\text{ }\mu\text{M}$ ($k_{\text{obs}} = 1 \times 10^{-4}\text{ s}^{-1}$) and $80\text{ }\mu\text{M}$ ($5 \times 10^{-4}\text{ s}^{-1}$), consistent with the active species retaining its dinuclear structure during the reaction. These k_{obs} values correspond to a 100-fold enhancement of the hydrolytic reaction rate compared to that of the uncatalyzed reaction. A similar enhancement was obtained with Fe^{3+} /EDDA for hydrolysis of 4-nitrophenyl phosphate.¹⁴ ^{31}P NMR of the final solution has revealed interactions between the complex and the reaction product,

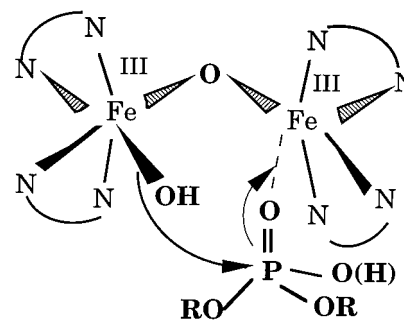


Figure 3. Proposed intermediate for hydrolysis of phosphodiester catalyzed by complex **3**.

suggesting that the rate-limiting step is likely to be the release of the reaction product. Interestingly, the reaction was catalytic with the total conversion of $200\text{ }\mu\text{M}$ BDNPP in the presence of $65\text{ }\mu\text{M}$ complex **1** at pH 6 in 3 h whereas the uncatalyzed reaction afforded only less than 10% conversion.¹⁵

We propose that complex **3** is the active species as it provides both an exchangeable site for phosphodiester binding and a nucleophilic hydroxo group on the adjacent iron site. Substrate binding is supported by ^{31}P NMR and UV–visible spectroscopies and by kinetic experiments showing a saturation behavior for BDNPP ($K_{\text{m}} = 90\text{ }\mu\text{M}$).¹⁶ The hydroxo ligand, then close to the bound substrate, is the best candidate for an intramolecular reaction with the phosphorus atom and the nucleophilic displacement of the phenolate anion (Figure 3). Complexes **2** and **1** are much less reactive because they lack the water-exchangeable ligand and the OH nucleophilic group, respectively.

Here we have described the first (μ -oxo)diferric unit containing two stable hydroxo ligands in water. Its acid conjugate was found to be catalytically active during hydrolysis of phosphodiester, even though the reaction rate remains to be optimized. It thus mimics the activity of PAP, which is optimally active under weakly acidic conditions.⁵ Our results suggest that the enzyme has a similar mechanism and that PAP has selected nonheme dinuclear iron centers for their specific ability to (i) deprotonate water due to Lewis acidity of iron(III) and (ii) to provide a nucleophilic OH group adjacent to a coordinated phosphoester in a weakly acidic medium.^{4,17}

Supporting Information Available: For complex **2**, tables of crystal data, structure refinement details, positional parameters, anisotropic displacement parameters, and bond lengths and angles, and a unit cell diagram, a potentiometric titration curve for **1**, text giving the experimental conditions for the potentiometric titration, and a table listing initial rates and K_{obs} values as a function of pH (10 pages). Ordering information is given on any current masthead page.

IC9711877

(14) Sadler, N. P.; Chuang, C. C.; Milburn, R. M. *Inorg. Chem.* **1995**, *34*, 402–404.

(15) The k_{obs} of the uncatalyzed hydrolysis has been reported equal to $2.1 \times 10^{-6}\text{ s}^{-1}$: Kirby, A. J.; Jencks, W. P. *J. Am. Chem. Soc.* **1965**, *87*, 3209–3216.

(16) Only at pH under 6.5 did BDNPP addition to complex **1** lead to a blue shift of the low-energy UV–visible oxo to Fe LMCT band. In addition, ^{31}P NMR of an equimolar **1**–BDNPP complex recorded at $50\text{ }^{\circ}\text{C}$ shows that only under pH 6.5 did the phosphorus resonance characteristic of free BDNPP disappear, in accordance with the interaction of the phosphodiester with the magnetic iron atom.

(17) Vincent, J. B.; Crowder, M. W.; Averill, B. A. *Trends Biochem. Sci.* **1992**, 105–110.